Determination of Optical Constants of Nanocluster CdO Thin Films Deposited by Sol–Gel Technique

Z. Serbetci[a], B. Gunduz[b], A.A. Al-Ghamdi[c], F. Al-Hazmic,[c], K. Arik[a],
F. El-Tantawy[d], F. Yakuphanoglu[c,e,*] and W.A. Farooq[f]

[a]Department of Chemistry, Faculty of Arts and Sciences, Bingol University, Bingol, Turkey

[b]Department of Science Education, Faculty of Education, Muş Alparslan University, 49100 Muş, Turkey

[c]Department of Physics, Faculty of Science, King Abdulaziz University, Jeddah 21589, Saudi Arabia

[d]Department of Physics, Faculty of Science, Suez Canal University, Ismailia, Egypt

[e]Department of Physics, Faculty of Science, Firat University, Elazig 23169, Turkey

[f]Department of Physics and Astronomy, College of Science, King Saud University, Riyadh, Saudi Arabia

The optical properties of the CdO and Pt doped CdO thin films synthesized by sol–gel technique were investigated. The lowest grain size value (81.34 nm) was found to be for CdO thin film. The Pt doped CdO films are transformed to clusters with nanoparticles. The transparency properties of the CdO thin film is changed with Pt doping. The plots of refractive index indicate abnormal and normal dispersion regions. The refractive index values of the CdO thin film are changed with Pt doping. The direct optical band gap values of the films were changed with doping of Pt. The film of 0.5% Pt doped CdO indicates the lowest optical band gap value (2.421 eV). The imaginary parts of the optical conductivity of the CdO and Pt doped CdO thin films are higher than that of the real parts of the optical conductivity.

1. Introduction

In recent years, there have been many works on the production and investigation of the physical properties of transparent conducting oxide (TCO) materials due to their electrical and optical properties such as low resistivity and high optical transmittance [1–5]. The first report of a TCO was published in 1907, when Badeker reported that thin films of Cd metal deposited in a glow discharge chamber could be oxidized to become transparent while remaining electrically conducting [5]. Since then, the commercial value of TCO thin films has been recognized [5], and the list of potential TCO materials has expanded with doping of various materials [6]. TCOs have great importance in the semiconductor, electronic and optoelectronic devices [7]. Thin films of n-type transparent conducting oxides (n-TCOs) such as zinc oxide (ZnO) [8], cadmium oxide (CdO) [9–11], indium oxide (In_2O_3) [12], tin oxide (SnO_2) [13], indium tin oxide (ITO) [14] and p-type transparent conducting oxides (p-TCOs) such as $CuAlO_2$ [15, 16], $SrCu_2O_2$ [17], tin–gallium oxide [18], etc. have received considerable attention mainly due to their important potential applications, which include photovoltaic solar cells, gas sensors, transparent electrodes, and other optoelectronic devices [7].

TCO thin films such as ZnO, InO, SnO_2, ITO and CdO have attracted considerable attention because of their low resistivity and high optical transmittance [1–5]. TCOs are used due to their optical, sensitive to light and electrical properties, for photodiodes, solar cells, smart windows, flat panel display and light emitting, surface acoustic wave device, varistors, photovoltaic materials, liquid crystal displays, gas sensors, transparent conducting electrodes, phototransistors, optical heaters etc. other optoelectronic applications [6, 19–27]. The high conductivity of TCO films results mainly from stoichiometric deviation. The conduction electrons in the TCO films are supplied from donor sites associated with oxygen vacancies or excess metal ions [28]. The oxide is insoluble in water, absorbs CO_2 from air and can be reduced to the conducting oxides which have received very little attention; though it is one of the promising candidate for optoelectronic field [5, 29–31].

Among different TCOs, CdO is considered as a promising material for photovoltaic applications due to its high electrical conductivity and optical transmittance in the visible region of solar spectrum [32] and CdO is particularly interesting due to its low resistivity and high carrier concentration, which endows it great potential for using in optoelectronic devices [6, 33, 34]. CdO based TCOs are of great interest due to their metal like charge transport behavior with an exceptionally large carrier mobility and good optical transparency in the visible region [35–37]. The CdO has special features such as high conductivity, high transmission, and low band gap which made it applicable in photodiodes, solar cells, flat panel displays, smart windows, optical communications, thin-film resistors, phototransistors, photovoltaics, transpar-

---

*corresponding author; e-mail: fyhanoglu@firat.edu.tr

ent conducting electrodes, liquid crystal displays, IR detectors, and antireflecting coatings [5, 30, 31, 38]. Due to its low optical band gap, non-stoichiometric undoped CdO is not widely used in optoelectronics and photovoltaics, although CdO thin films show low resistivity due to defects of oxygen vacancies and cadmium interstitials [24, 34]. CdO is an *n*-type semiconductor with a NaCl (a rock-salt crystal structure (fcc)) structure [27] and band gap values of 2.5 eV [39], 2.2–2.8 eV [40–42], 2.16 eV [40], 2.2–2.4 eV [43], between 2.2 and 2.7 eV [8, 41, 44, 45] and has a direct energy band gap of 2.2 eV [46, 47], in-between 2.2 and 2.7 eV [8, 24, 41, 45, 48], narrow energy band gap energy (2.6 eV and 2.1 eV direct and indirect band gap, respectively) [48], direct band gap of 2.5 eV, indirect band gap of 2.1 eV [48], two indirect bandgaps at 1.18–1.2 eV and 0.8–1.12 eV [8, 24, 41, 45, 48] and a relatively low intrinsic band gap of 2.3 eV [49] and a resistivity of 10^{-2}–10^{-4} Ω cm [40–42].

Theoretically, it was established that CdO has a direct band gap of 2.18 eV [45] or 2.38 eV [50] and two indirect band gaps of 0.8 eV and 1.2 eV [51] or 0.95 eV and 1.11 eV [52], or 1.12 eV and 1.18 eV [53]. The *n*-type conduction of undoped CdO was attributed to its native oxygen vacancies and cadmium interstitials [54]. CdO shows very high electrical conductivity even without doping due to the existence of shallow donors caused by intrinsic interstitial cadmium atoms and oxygen vacancies [1, 46]. CdO films are transparent in visible and near infrared (NIR) spectral regions and have an electrical resistivity of 10^{-2}–10^{-4} Ω cm [44].

Researchers are trying to modify the synthesis procedure for CdO thin films with the aim to improve chemical and physical properties of this material and try to synthesize nanostructures with well defined geometrical shapes (e.g., spheres, cubes, rods, wires, tubes, tetrapods, ribbons, disks, and platelets). Researchers effort to organize them as 2- and 3-dimensional assemblies has further expanded the possibility of developing new strategies for light energy conversion. The first six shapes are being intensively studied for renewable energy applications [55–57]. CdO thin films have great technological interest due to their high-quality electrical and optical properties [58]. Doped CdO films, as multi component oxides films constituted of CdO, have been used in several applications: photovoltaic devices [59, 60], gas sensors [61], phototransistors and diodes [62], etc.

Different physical and chemical deposition methods have been employed to prepare undoped CdO and doped CdO films such as ion beam sputtering, successive ionic layer adsorption and reaction (SILAR), thermal evaporation, metal organic chemical vapor deposition (MOCVD), sputtering, electron beam evaporation and sol–gel, spray pyrolysis, dc magnetron sputtering, radio frequency (rf) sputtering, chemical bath deposition, pulsed laser deposition (PLD) etc. [7, 33, 42, 63–71]. Among these methods of preparation of pure and doped CdO, the sol–gel technique is one of the most promising tools in material science and it is one of the most promis-

ing available methods for synthesizing nanoparticles of controlled size and morphology [72]. The sol–gel spin coating method has various advantages such as cost effectiveness, thin, transparent, multicomponent oxide layers of many compositions on various substrates, simplicity, excellent compositional control, homogeneity and lower crystallization temperature [28]. Also, it does not require vacuum apparatus and has the potential to produce films with large areas on various substrates [73]. The synthetic route provided by this system is the most feasible one for designing materials possessing unique properties. Generally, it is a process concerning transition of a system from liquid "sol" (the colloidal suspension of particles) into solid "gel" [72].

However, there are few works reported in the literature with respect to CdO films obtained by the sol–gel technique, a fact rather surprising due to these excellent advantages that the sol–gel technique presents [48]. The optical properties and thus the band gap of CdO can also be controlled by doping [74]. Some researchers reported that CdO films can be doped with Sc, Y, Sm, Mn, Sn, Mg, Cu, F, In, Ga, Al, Fe, Cd, Zn, Ti, Dy, etc. [27, 33, 39, 54, 58, 67, 71, 75–77] and they have been used in several applications: photovoltaic devices, gas sensors, phototransistors, and diodes, etc. [58, 67]. It is found that the doping of In, Ti, Al enhances E_g to 2.74–2.84 eV and simultaneously increases the electrical conductivity [27, 34, 39]. Maity and Chattopadhyay [78] have reported that the band gap of CdO can be reduced by Al doping, whereas Deokate et al. [79] have reported that F doping increases the optical band gap of pure CdO films. It was observed that the band gap of the CdO film decreases from 2.76 to 2.36 eV due to increase in the Al percentage from 1.32 to 7.24. Yakuphanoglu [80] reported that the electrical, structural and optical properties of CdO films could be controlled by boron dopant for electronic and photovoltaic applications.

Recently, Dakhel [76, 81, 82] has published a few papers based on rare earth element doped CdO films. It is reported in these papers that the optical band gap of the CdO films in general decreases due to light doping of rare earth elements [74]. Gupta et al. reported the effect of growth parameters on structural, optical, and electrical properties of Ti, Sn, Al doped CdO thin films by pulse laser deposition technique [83–86]. Martin et al. [87] have deposited multilayer of TCOs using Sn doped CdO and Sn doped $CdIn_2O_4$ using pulsed laser deposition technique. It was found that doping of CdO with ions of a smaller ionic radius than that of Cd^{2+}, like In, Sn, Al, Sc, and Y improved its electrical conductivity and increased its optical energy gap, which was explained by application of Moss–Burstein (B–M) effect [11, 24, 75, 78, 82, 88, 89]. Gupta et al. [74] reported that the bandgap of the CdO film is decreased by Cu doping and among the Cu doped CdO films, the bandgap was observed to increase with increase in copper doping level.

Furthermore, some scientists made many researches on optical properties on the pure CdO and doped CdO thin

films. Yakuphanoglu [90] reported that the transparency of the nanocluster–CdO film lies in the range of 70–80% in the visible range and it reaches a 92% value in the visible range and with its optical band gap E_g of 2.27 eV. Dakhel [91] reported that the CdO and Tl-doped CdO films with the optical energy band values of 2.308 eV and 2.721 eV, respectively. Kose et al. [1] reported that the CdO and In-doped CdO films with the optical band gap values of 2.51, 2.49, 2.62 and 2.78 eV, the refractive index values of 4.39, 3.86, 2.93 and 2.05 at $\lambda = 600$ nm for pure CdO, 1%, 3%, and 5% In-doped CdO films, respectively. Gupta et al. [74] reported the CdO and Cu-doped CdO films with the optical band gap values of 2.57, 2.41, 2.47, 2.49 and 2.52 eV for pure CdO, 1%, 2%, 3% and 4% Cu-doped CdO films, respectively. Yakuphanoglu et al. [28] reported the CdO films with the optical band gap of 2.45 eV. Dakhel [54] reported the CdO and Ga-doped CdO films with the optical band gap values of 2.16, 2.22, 3.70 and 2.17 eV for pure CdO, 3%, 6% and 9% Ga doped CdO films, respectively. Zheng et al. [34] reported the CdO and Sn-doped CdO films with the optical band gap values of 2.40 and 2.82–2.93 eV for pure CdO and Sn–CdO thin films, respectively. Yakuphanoglu [80] reported the CdO and boron-doped CdO thin films with the optical band gap values of 2.27, 2.17, 2.45, 2.29 and 2.24 eV, the dispersion energy values of 7.17, 1.85, 27.55, 5.34 and 7.01 eV, the average excitation energy values of 3.79, 3.03, 12.03, 3.31 and 4.74 eV, an average oscillator wavelength values of 327.7, 409.9, 103.2, 375.2 and 262 nm, the average oscillator strength values of 1.75×10^{13}, 3.64×10^{12}, 2.13×10^{13}, 1.13×10^{13} and 2.13×10^{13} m^{-2} for pure CdO and 1%, 5%, 10% and 15% B doped CdO thin films, respectively. Santos-Cruz et al. [70] reported the CdO and fluorine (F)-doped CdO films with the optical band gap values of about 2.65, 2.70, 2.77, and 2.82 eV for pure CdO and 1%, 5%, and 20% F-doped CdO thin films, respectively.

In this work we have employed sol–gel technique to prepare platinum (Pt) doped CdO. There is no any report on the preparation, surface morphology and optical properties of Pt doped cadmium oxide thin films by sol–gel technique. In this study, we have studied in detail the surface morphology and optical properties of the pure CdO and Pt doped CdO thin films synthesized by sol–gel technique which is a very simple and economical method.

2. Experimental details

Thin films of platinate doped CdO were fabricated using the sol–gel technique. Cadmium acetate dehydrate ($C_4H_6CdO_4 2(H_2O)$), potassium hexachloroplatinate(IV) (Pt), 2-metoxyethanol and monoethanolamine were used for fabrication of CdO and Pt doped CdO films. The required chemicals were purchased from Alfa Aesar and were used without further purification. In a typical synthesis, 0.5 M of cadmium acetate dehydrate was slowly dissolved in 2-metoxyethanol followed by addition of monoethanolamine. The molar ratio of monoethanolamine

to cadmium acetate was 1.0. For Pt doped CdO, the required amount of potassium hexachloroplatinate was added in the above mixture to get 0.1%, 0.5%, 1% and 2% of Pt doped CdO. The prepared mixtures were stirred using a magnetic stirrer at 60 °C for about 30 min to obtain clear homogeneous solution and then the sol was kept for aging for 4 h before the film deposition. The pure CdO and Pt doped CdO films were deposited on microscopy glasses at 1500 rpm for 30 s by the sol–gel spin coating method. After the spin coating, the films were dried at 150 °C for 5 min to evaporate the solvent and remove organic residuals. This coating/drying procedure was repeated for eight times. Then, the prepared undoped and Pt doped CdO films were annealed at 400 °C for 1 h in a furnace. Surface morphology was investigated by PARK system XE100E atomic force microscopy (AFM). The absorbance, transmittance and reflectance properties of the films were taken using a Shimadzu UV-vis-NIR3600 spectrophotometer.

3. Results and discussion

3.1. Surface morphology properties of Pt–doped CdO films

X-ray diffraction patterns of Pt–doped CdO films are shown in Fig. 1a. It is evaluated that undoped CdO and Pt doped CdO films have the cubic NaCl structure with the lattice parameters of undoped CdO consented with JCPDS data [92]. The obtained results suggest that [111] direction is the direction preferred orientation growth. This means that the CdO films are grown along this direction. The intensity of the (111) plane is changed with Pt content. This indicates that Pt ions substitutionally replaced Cd ions in the lattice.

The surface morphology properties of the active layers of the CdO and Pt doped CdO thin films were investigated using an AFM. The all images of the CdO thin film were taken in 5 μm $\times$ 5 μm area. Figure 1 b–f shows one-dimensional (1D) AFM images of the CdO and Pt doped CdO thin films for 5 μm $\times$ 5 μm area. As seen in Fig. 1, the CdO, 0.5% Pt–CdO, 1% Pt–CdO, and 2% Pt–CdO thin film are formed from small crystal grains and 0.1% Pt–CdO thin film is formed from nanoclusters, with an almost homogeneous distribution.

TABLE I

The crystal grain/nanocluster size and surface roughness R_q values of the CdO and Pt doped CdO thin films for 5 μm $\times$ 5 μm area.

Thin films	Grain/nanocluster size [nm]	Surface roughness (R_q) [nm]
pure CdO	81.34	35.215
0.1% Pt–CdO	816.5	128
0.5% Pt–CdO	396.91	71.334
1% Pt–CdO	373.9	71.562
2% Pt–CdO	206.2	30.724
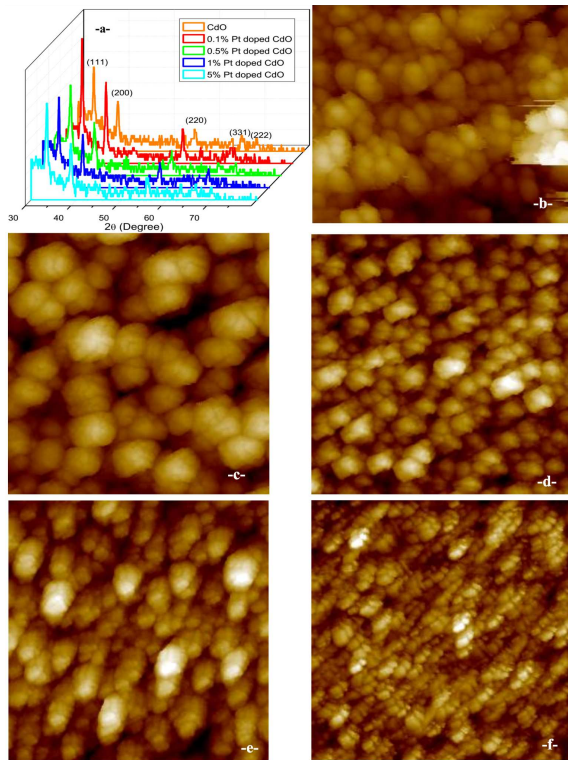
Fig. 1. One-dimensional (1D) AFM images of the (a) pure CdO, (b) 0.1%, (c) 0.5%, (d) 1% and (e) 2% Pt doped CdO thin film for 5 μm × 5 μm area.

The small crystal grain and nanocluster size values of the CdO and Pt doped CdO thin films for 5 μm × 5 μm area were determined and given in Table I. The surface roughness R_q values of the CdO and Pt doped CdO thin films for 5 μm × 5 μm area were determined from the all surfaces of the CdO and Pt doped CdO thin films using Park System XEI software programming and given in Table I. As seen in Table I, the average crystal grain size value (81.34 nm) of the CdO thin film is the lowest value of all the films, while the average crystal grain size value (396.91 nm) of the 0.5% Pt–CdO thin film is the highest value of all films. Also, the nanocluster size value of the 0.1% Pt–CdO thin film was found to be 816.5 nm. It is observed that the small crystal grain size of the CdO thin film increases with doping of Pt. As seen in Table I, the R_q value (30.724 nm) of the 2% Pt–CdO thin film is the lowest value of all the films, while the surface roughness (R_q) value (128 nm) of the 0.1% Pt–CdO thin film is the highest value of all films. Therefore, the grain size and the surface roughness of the co-doped films could be controlled.

3.2. Optical properties of Pt doped CdO thin films

3.2.1. Determination of refractive index parameters of the CdO and Pt doped CdO thin films

The transmittance spectra of the CdO and Pt doped CdO thin films were measured to investigate their optical properties and they are shown in Fig. 2a. In the visible region, the average transmittance values of the CdO and Pt doped CdO thin films were calculated and given in Table II. As seen in Table II, the average transmittance (71.316%) of the CdO thin film is the highest value, while the average transmittance (50.461%) of the 0.5% Pt–CdO thin film is the lowest value of all the films. This value is close to value (70–80%) of the transparency in the visible range in the literature [90]. As seen in Table II, the average transmittance value of the CdO thin film decreases with doping of Pt. To estimate the absorption band edge of the CdO and Pt doped CdO thin films, the first derivative of the optical transmittance can be computed. The curves of $dT/d\lambda$ versus wavelength were plotted, as shown in Fig. 2b. As seen in Fig. 2b, the maximum peak position corresponds to the absorption band edge and there is a small shift in the direction of the longer wavelengths. The absorption band edge values of the CdO and Pt doped CdO thin films were calculated from the maximum peak position and given in Table II. As seen in Table II, the maximum peak values of the CdO and Pt doped CdO thin films vary from 548.5 to 637.5 nm. This suggests that the absorption band edge values of the CdO and Pt doped CdO thin films shift from 2.264 to 1.948 eV with the doping of Pt. As seen in Table II, the absorption band edge of the CdO thin film decreases with doping of Pt.
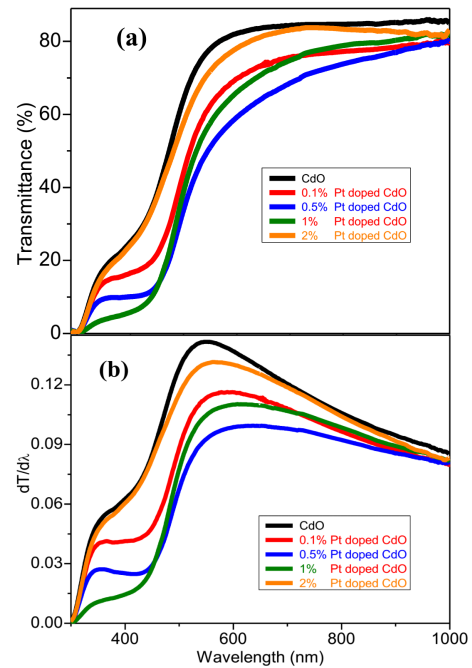
Fig. 2. (a) The transmittance spectra and (b) the curves of $dT/d\lambda$ versus wavelength of the CdO and Pt doped CdO thin films.

TABLE II

Some important optical parameters of the CdO and Pt doped CdO thin films.

	Pure CdO	0.1% Pt–CdO	0.5% Pt–CdO	1% Pt–CdO	2% Pt–CdO
average transmittance [%]	71.316	58.745	50.461	55.086	68.446
maximum peak [nm]	548.5	598	637.5	607	561.5
absorption band edge [eV]	2.264	2.077	1.948	2.046	2.212
E [eV]	2.835	2.782	2.695	2.829	3.670
E_d [eV]	1.648	3.678	4.733	2.869	2.363
E_d/E	0.581	1.322	1.756	1.014	0.644
n_∞	1.343	1.846	1.974	1.702	1.211
λ [nm]	438.1	446.5	460.9	439.1	338.4
S [m^{-2}] $\times 10^{12}$	4.074	12.08	13.64	9.838	4.187

Fig. 3. The reflectance spectra of the CdO and Pt doped CdO thin films.
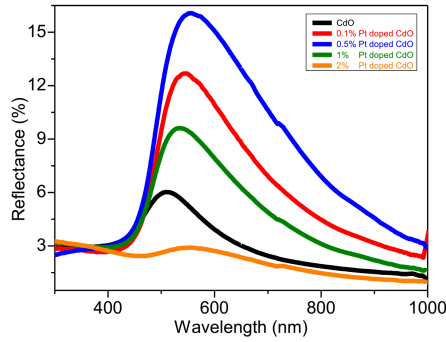
Fig. 4. The refractive index plot vs. wavelength of the CdO and Pt doped CdO thin films.

The reflectance spectra of the CdO and Pt doped CdO thin films is shown in Fig. 3. As seen in Fig. 3, reflectance spectra of the CdO thin films changes with doping of Pt and the reflectance spectra of the 0.5% Pt–CdO thin film is the highest value, while the reflectance spectra of the 2% Pt–CdO thin film is the lowest value of all the films.

The refractive index is an important parameter for optical applications. Thus, it is important to determine optical constants of the CdO and Pt doped CdO thin films and the complex optical refractive index of the films is expressed as

$$\hat{n} = n(\omega) + \mathrm{i}k(\omega), \tag{1}$$

where n is the real part and k is the imaginary part of complex refractive index. The optical properties of the films are characterized by refractive index. The refractive index of the films can be obtained from the following equation [93]:

$$n = \left\{ \left[\frac{4R}{(R-1)^2} - k^2 \right]^{1/2} - \frac{R+1}{R-1} \right\}. \tag{2}$$

The refractive index values of the CdO and Pt doped CdO thin films were calculated from Eq. (2).

Figure 4 shows the refractive index plot vs. wavelength of the CdO and Pt doped CdO thin films. As seen in Fig. 4, plot of refractive index is composed of two regions so-called abnormal and normal dispersion. The n values of the CdO and Pt doped CdO thin films increase with increasing λ in abnormal dispersion region, while the re-

fractive index (n) values of the CdO and Pt doped CdO thin films decrease with increasing wavelength in normal dispersion region. As seen in Fig. 4, the refractive index values of the CdO thin film change with doping of Pt and the refractive index of the 0.5% Pt–CdO thin film is the highest value, while the refractive index of the 2% Pt–CdO thin film is the lowest value of all the films. This suggests that the refractive index of the CdO thin film can be both reduced and increased with doping of Pt. This is a very significant improvement for optical applications. The refractive index (2.269) of the 0.5% Pt–CdO thin film at $\lambda = 600$ nm is higher than that value (2.05) of the 5% In-doped CdO films at $\lambda = 600$ nm in the literature [1], but the refractive index values (between 2.93 and 4.39) of the CdO and In-doped CdO films at $\lambda = 600$ nm in the literature [1] is higher than that of the studied pure CdO, 0.1%, 1% and 2% Pt–CdO thin film at $\lambda = 600$ nm
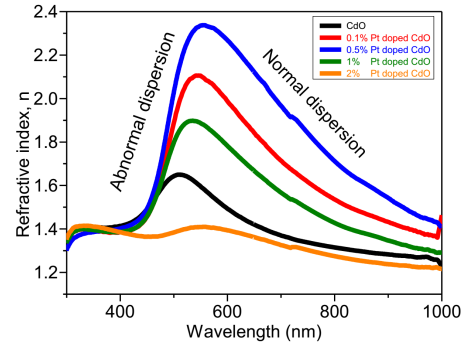
The refractive index dispersion in polymer can be analyzed using single oscillator model. The dispersion of the refractive index is expressed as [94]:

$$n^2 - 1 = \frac{E_\mathrm{d}E_0}{E_0^2 - E^2}, \tag{3}$$

where h is Planck's constant, ν is the frequency, E is the photon energy, E_0 is the average excitation energy for electronic transitions, and E_d is the dispersion energy, which is a measure of the strength of inter band optical transitions. Experimental verification of Eq. (3) [single-oscillator model] can be obtained by plotting $1/(n^2 - 1)$

vs. E^2. The resulting straight line yields values of the parameters E_0 and E_d.

The plot $1/(n^2 - 1)$ vs. E^2 of the CdO and Pt doped CdO thin films is shown in Fig. 5.
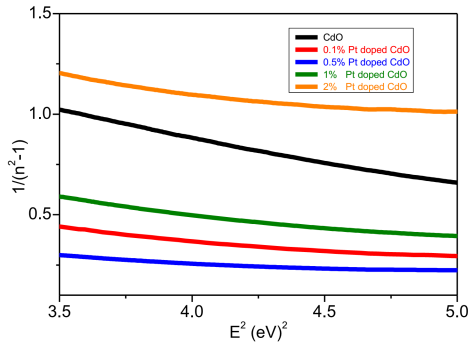
Fig. 5. The plot $1/(n^2 - 1)$ vs. E^2 of the CdO and Pt doped CdO thin films.

The E_0 and E_d values of the CdO and Pt doped CdO thin films were calculated for normal dispersion regions of the films and given in Table II. As seen in Table II, the excitation and dispersion energy values of the CdO thin film change with doping of Pt. The excitation energy value (2.695 eV) of the 0.5% Pt–CdO thin film is the lowest value of all the films, while the excitation energy value (3.670 eV) of the 2% Pt–CdO thin film is the highest value of all the films. This suggests that the excitation energy of the CdO thin film can be both reduced and increased with doping of Pt. The excitation energy values (2.835 eV and 2.829 eV, respectively) of the CdO and 1% Pt doped CdO thin films are lower than these values (3.79 eV and 3.03 eV, respectively) of the pure CdO and 1% B doped CdO thin films in the literature [80]. Similarly, the dispersion energy value (1.648 eV) of the pure CdO thin film is the lowest value of all the films, while the dispersion energy value (4.733 eV) of the 0.5% Pt–CdO thin film is the highest value of all the films. This suggests that the dispersion energy of the CdO thin film can be increased with doping of Pt. The dispersion energy value (1.648 eV) of the CdO thin film is lower than that value (7.17 eV) of the pure CdO thin film in the literature [80], while the dispersion energy value (2.869 eV) of the 1% Pt doped CdO thin film is higher than that value (1.85 eV) of the 1% B doped CdO thin films in the literature [80]. As seen in Table II, the E_d/E_0 ratio (1.756) of the 0.5% Pt–CdO thin film is the highest value of all the films, while the E_d/E_0 ratio (0.581) of the pure CdO thin film is the lowest value of all the films. This suggests that the E_d/E_0 ratio of the CdO thin film can be increased with doping of Pt.

The refractive index can be also analyzed using the following relation [94]:

$$\frac{n_\infty^2 - 1}{n^2 - 1} = 1 - \left(\frac{\lambda_0}{\lambda}\right)^2, \tag{4}$$

where n_∞ is the long wavelength refractive index and λ_0 is the average oscillator wavelength. The n_∞ and λ_0 values of the CdO and Pt doped CdO thin films were obtained from the linear part of plotted $1/(n^2-1)$ vs. λ^{-2} curve (Fig. 6) and were calculated and given in Table II. As seen in Table II, the n_∞ and λ_0 values of the CdO thin film change with doping of Pt. The n_∞ value (1.211) of the 2% Pt–CdO thin film is the lowest value of all the films, while the n_∞ value (1.974) of the 0.5% Pt–CdO thin film is the highest value of all the films. This suggests that the n_∞ of the CdO thin film can be both reduced and increased with doping of Pt. The n_∞ value (1.343) of the CdO thin film is lower than that value (1.7) of the pure CdO thin film in the literature [80], while the n_∞ value (1.702) of the 1% Pt doped CdO thin film is higher than that value (1.27) of the 1% B doped CdO thin film in the literature [80]. Similarly, the λ_0 value (338.4 nm) of the 2% Pt–CdO thin film is the lowest value of all the films, while the λ_0 value (460.9 nm) of the 0.5% Pt–CdO thin film is the highest value of all the films. This suggests that the λ_0 value of the CdO thin film can be reduced and increased with doping of Pt. The λ_0 values (438.1 nm and 439.1 nm, respectively) of the CdO and 1% Pt doped CdO thin films are higher than those values (327.7 nm and 409.9 nm, respectively) of the pure CdO and 1% B doped CdO thin films in the literature [80].
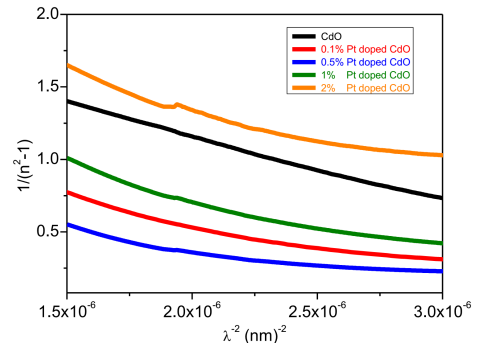
Fig. 6. The plot $1/(n^2 - 1)$ vs. λ^{-2} of the CdO and Pt doped CdO thin films.

Rearranging of Eq. (4) gives

$$n^2 - 1 = \frac{S_0 \lambda_0^2}{1 - \lambda_0^2/\lambda^2}, \tag{5}$$

where $S_0 = (n_\infty^2 - 1)/\lambda_0^2$. The S_0 values of the CdO and Pt doped CdO thin films were calculated and given in Table II. As seen in Table II, the S_0 value (1.324×10^{12} m^{-2}) of the CdO thin film increases with doping of Pt. The S_0 value (4.074×10^{12} m^{-2}) of the CdO thin film is lower than that value (1.75×10^{13} m^{-2}) of the pure CdO thin film in the literature [80], while the S_0 value (9.838×10^{12} m^{-2}) of the 1% Pt doped CdO thin film is higher than that value (3.64×10^{12} m^{-2}) of the 1% B doped CdO thin film in the literature [80].

3.2.2. Optical band gap properties of the CdO and Pt doped CdO thin films

The optical band gap of optical transitions can be obtained dependence of absorption coefficient on photon

energy. It is evaluated that the band structure of the film obeys the rule of direct transition and in a direct band gap material; the absorption coefficient dependence on photon energy is analyzed by the following relation [93, 95]:

$$\alpha = A(h\nu - E_{\rm g})^m, \tag{6}$$

where A is a constant, $h\nu$ is the photon energy, $E_{\rm g}$ is the optical band and m is the parameter measuring type of band gaps.
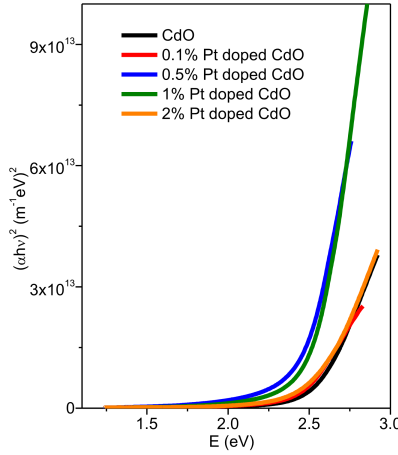
Fig. 7. The dependence of photon energy E of $(\alpha h\nu)^2$ of the CdO and Pt doped CdO thin films.

To determine the optical band gap of the CdO and Pt doped CdO thin films, the dependence of photon energy E of $(\alpha h\nu)^2$ of the CdO and Pt doped CdO thin films is shown in Fig. 7. As seen in inset of Fig. 7, there is a linear region for the direct band gap of the CdO and Pt doped CdO thin films.

TABLE III

The direct band gap values of the CdO and Pt doped CdO thin films.

Thin films	E_{gd} [eV]
pure CdO	2.524
0.1% Pt–CdO	2.446
0.5% Pt–CdO	2.421
1% Pt–CdO	2.496
2% Pt–CdO	2.506

By extrapolating the linear plot to $(\alpha h\nu)^2 = 0$, a direct energy-gap values of the CdO and Pt doped CdO thin films were obtained and given in Table III. As seen in Table III, the direct energy-gap values of the CdO thin film change with doping of Pt. The direct energy--gap value (2.524 eV) of the CdO thin film is the highest value of all the films, while the direct energy-gap value (2.421 eV) of the 0.5% Pt–CdO thin film is the lowest value of all the films. This suggests that the direct energy-gap of the CdO thin film can be decreased with doping of Pt and the electrical conductivity of the CdO thin film can be increased with convenient doping of Pt. The direct energy-gap value (2.524 eV) of the CdO thin

film is higher than that the values (2.18, 2.2, 2.3, 2.38 eV) of CdO film in the literature [45–47, 50, 96]. Also, the direct energy-gap value (2.524 eV) of the CdO thin film is close to values (2.6 eV) of the direct energy-gap in the literature [48].

3.2.3. Dielectric and electrical susceptibility properties of the CdO and Pt doped CdO thin films

The complex dielectric constant is described as

$$\hat{\varepsilon} = \varepsilon_1 + {\rm i}\varepsilon_2 = \hat{n}^2 = (n \pm {\rm i}k)^2 = (n^2 - k^2) + {\rm i}2nk, \tag{7}$$

where ε_1 is the real part and ε_2 is the imaginary of the dielectric constant. The imaginary and real parts of dielectric constant are given as [97]:

$$\varepsilon_1 = n^2 - k^2 \tag{8}$$

and

$$\varepsilon_2 = 2nk, \tag{9}$$

where $k = \alpha\lambda/4\pi$. Figure 8a,b shows the real and imaginary parts of dielectric constant dependence on photon energy, respectively. As seen in Fig. 8a, plot of the real part of dielectric constant is composed of two regions between about 1.24 eV and 3.05 eV which they called normal and abnormal dispersion region. The ε_1 values of the CdO and Pt doped CdO thin films increase with increasing photon energy (or frequency) in normal dispersion region, while the ε_1 values of the CdO and Pt doped CdO thin films decrease with increasing photon energy (or frequency) in abnormal dispersion region. As seen in Fig. 8a, the ε_1 values of the CdO thin film change with doping of Pt and in between about 1.24 eV and 3.05 eV region, the ε_1 of the 0.5% Pt–CdO thin film is the highest value, while the ε_1 of the 2% Pt–CdO thin film is the lowest value of all the films. This suggests that the ε_1 of the CdO thin film can be both reduced and increased with doping of Pt. As seen in Fig. 8b, the imaginary part (ε_2) of dielectric constant increases with E until about 4.55 eV, then it decreases with increasing photon energy (E). As seen in Fig. 8a,b, the real parts of the dielectric constant of the CdO and Pt doped CdO thin films are higher than that of imaginary parts of the dielectric constant.

The susceptibility associated with electron transitions from band i to band j is expressed as [98]:

$$\chi_\nu = \frac{e^2}{4\pi^2 m} \sum_k \frac{f_{jik}}{\nu_{jik}^2 - \nu^2}, \tag{10}$$

where k is the wave number vector, $h\nu_{jik}$ is the energy difference between the state k in band i and the state k in band j and f_{jik} is the oscillator strength for this transition. The electrical susceptibility due to the intraband transitions of free carriers can be obtained from the optical constants and it is determined as [99]:

$$\chi_{\rm c} = \frac{1}{4\pi}(n^2 - k^2 - \varepsilon_0), \tag{11}$$

where ε_0 is the dielectric constant in the absence of any contribution from free carriers. The electric susceptibility of the CdO and Pt doped CdO thin films dependence of photon energy is shown in Fig. 9. As seen in Fig. 9, the electric susceptibility ($\chi_{\rm c}$) of the CdO and Pt doped
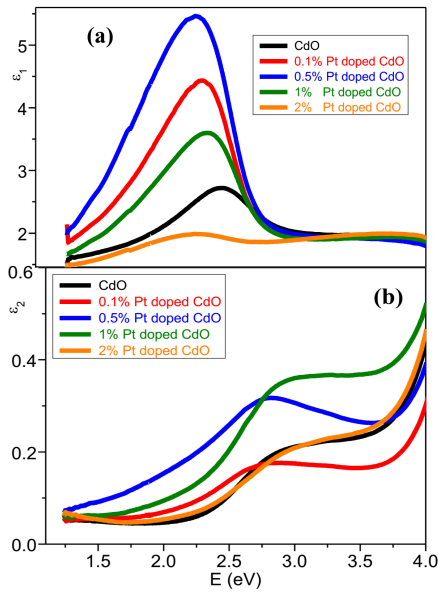
Fig. 8. The (a) real and (b) imaginary parts of dielectric constant of the CdO and Pt doped CdO thin films dependence on photon energy.
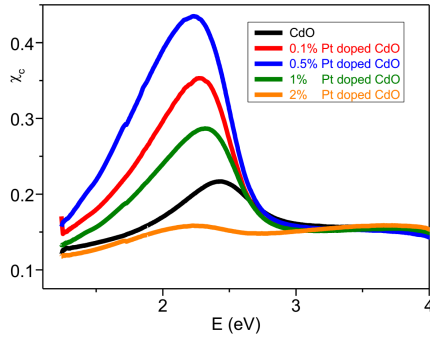
Fig. 9. The electric susceptibility of the CdO and Pt doped CdO thin films dependence of photon energy.

CdO thin films is composed of two regions for between about 1.24 eV and 3.05 eV and the χ_c values of the CdO thin film change with doping of Pt and in between about 1.24 eV and 3.05 eV region. The χ_c of the 0.5% Pt–CdO thin film is the highest value, while the χ_c of the 2% Pt–CdO thin film is the lowest value of all the films. This suggests that the χ_c of the CdO thin film can be both reduced and increased with doping of Pt.

3.2.4. Optical conductivity properties of the CdO and Pt doped CdO thin films

The optical properties of the CdO and Pt doped CdO thin films can be analyzed by a complex optical conductivity [93, 100]:

$$\sigma(\omega) = \sigma_1(\omega) + i\sigma_2(\omega), \qquad (12)$$

where σ_1 is the real part of conductivity and σ_2 is the imaginary part of conductivity.

The real part and imaginary parts of the optical conductivity of the CdO and Pt doped CdO thin films are shown in Fig. 10a,b, respectively. As seen in Fig. 10a, the
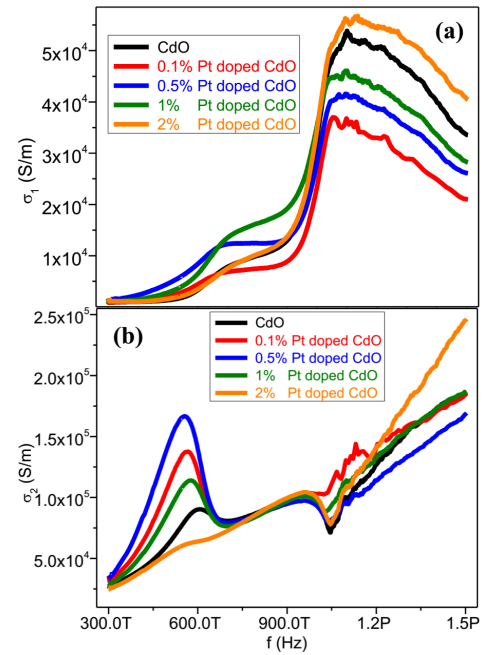
Fig. 10. The (b) real and (b) imaginary parts of the optical conductivity of the CdO and Pt doped CdO thin films dependence on frequency.

real part (σ_1) of the optical conductivity increases with frequency until about 1.09 THz, then it decreases with increasing frequency. As seen in Fig. 10b, there is a peak for between about 253 THz and 700 THz and the σ_2 values of the CdO thin film change with doping of Pt and in between about 253 THz and 700 THz region, the σ_2 of the 0.5% Pt–CdO thin film is the highest value, while the σ_2 of the 2% Pt–CdO thin film is the lowest value of all the films. This suggests that the σ_2 of the CdO thin film can be both reduced and increased with doping of Pt. As seen in Fig. 10a,b, the imaginary parts of the optical conductivity of the CdO and Pt doped CdO thin films are higher than that of the real parts of the optical conductivity.

4. Conclusions

The CdO and Pt doped CdO thin films were formed from small crystal grains with an almost homogeneous distribution. It was observed that the small crystal grain size of the CdO thin film increases with doping of Pt. Therefore, the grain size and the surface roughness of the co-doped films could be controlled. The absorption band edge values of the CdO and Pt doped CdO thin films shifted from 2.264 to 1.948 eV with the doping of Pt. The absorption band edge of the CdO thin film decreased with doping of Pt. The plot of refractive index is composed of two regions so-called abnormal and normal dispersion. The n values of the CdO and Pt doped CdO thin films increased with increasing λ in abnormal dispersion region, while the refractive index (n) values of the CdO and Pt doped CdO thin films decreased with increasing wavelength in normal dispersion region. The refractive index of the CdO thin film can be both reduced

and increased with doping of Pt. This is a very significant improvement for optical applications. The n_∞, λ_0, ε_1, χ_c, σ_2 and excitation of the CdO thin film can be both reduced and increased with doping of Pt. The dispersion energy and E_d/E_0 ratio of the CdO thin film can be increased with doping of Pt. Similarly, the S_0 value $(4.074 \times 10^{12} \text{ m}^{-2})$ of the CdO thin film increased with doping of Pt. The direct energy-gap of the CdO thin film can be decreased with doping of Pt and the electrical conductivity of the CdO thin film can be increased with convenient doping of Pt. The plot of the real part of dielectric constant was composed of two regions for between about 1.24 eV and 3.05 eV which they called normal and abnormal dispersion region. There was a peak for between about 253 THz and 700 THz and the σ_2 values of the CdO thin film changed with doping of Pt and in between about 253 THz and 700 THz region.

Acknowledgments

References

[1] S. Kose, F. Atay, V. Bilgin, I. Akyuz, *Int. J. Hydrogen Energy* **34**, 5260 (2009).

[2] L. Zhao, J. Lian, Y. Liu, Q. Jiang, *Appl. Surf. Sci.* **252**, 8451 (2006).

[3] F.O. Adurodija, L. Semple, R. Bruning, *Thin Solid Films* **492**, 153 (2005).

[4] I. Saadeddin, B. Pecquenard, J.P. Manaud, R. Decourt, C. Labrugère, T. Buffeteau, *Appl. Surf. Sci.* **253**, 5240 (2007).

[5] C.H. Bhosale, A.V. Kambale, A.V. Kokate, K.Y. Rajpure, *Mater. Sci. Eng. B* **122**, 67 (2005).

[6] B.G. Lewis, D.C. Paine, *MRS Bull.* **25**, 22 (2000).

[7] B. Saha, S. Das, K.K. Chattopadhyay, *Sol. En. Mater. Solar Cells* **91**, 1692 (2007).

[8] K.L. Chopra, S.R. Das, *Thin Film Solar Cells*, Plenum Press, New York 1983, Ch. 3, p. 346.

[9] G. Phatak, R. Lal, *Thin Solid Films* **245**, 17 (1994).

[10] A. Verkey, A.F. Fort, *Thin Solid Films* **239**, 211 (1994).

[11] A.J. Freeman, K.R. Poeppelmeier, T.O. Mason, R.P.H. Chang, T.J. Marks, *MRS Bull.* **25**, 45 (2000).

[12] C. Wang, V. Cimalla, G. Cherkashinin, H. Romanus, M. Ali, O. Ambacher, *Thin Solid Films* **515**, 2921 (2007).

[13] K.L. Chopra, S. Major, D.K. Pandya, *Thin Solid Films* **102**, 1 (1983).

[14] D.M. Mattox, *Thin Solid Films* **204**, 25 (1991).

[15] S. Gao, Y. Zhao, P. Gou, N. Chen, Y. Xie, *Nanotechnology* **14**, 538 (2003).

[16] A.N. Banerjee, K.K. Chattopadhyay, *J. Appl. Phys.* **97**, 084308 (2005).

[17] S. Sheng, G. Fang, C. Li, Z. Chen, S. Ma, L. Fang, X. Zhao, *Semicond. Sci. Technol.* **21**, 586 (2006).

[18] Y.X. Huang, Z.G. Ji, C. Chen, *Appl. Surf. Sci.* **253**, 4819 (2007).

[19] A.K. Kulkarni, K.H. Schulz, T.S. Lim, B. Khan, *Thin Solid Films* **345**, 273 (1999).

[20] N. Ito, Y. Sato, P.K. Song, A. Kaijio, K. Inoue, Y. Shigesato, *Thin Solid Films* **496**, 99 (2006).

[21] J.T. Lim, C.H. Jeong, A. Vozny, J.H. Lee, M.S. Kim, G.Y. Yeom, *Surf. Coat. Technol.* **201**, 5358 (2007).

[22] H. Kim, C.M. Gilmore, A. Pique, J.S. Horwitz, H. Mattoussi, H. Murata, Z.H. Kafafi, D.B. Chrisey, *J. Appl. Phys.* **11**, 6451 (1999).

[23] J.A.A. Selvan, A.E. Delahoy, S. Guo, Y.-M. Li, *Sol. En. Mater. Sol. Cells* **90**, 3371 (2006).

[24] Z. Zhao, D.L. Morel, C.S. Ferekides, *Thin Solid Films* **413**, 203 (2002).

[25] L.M. Su, N. Grote, F. Schmitt, *Electron. Lett.* **20**, 716 (1984).

[26] O. Gomez Daza, A.A.-C. Readigos, J. Campos, M.T.S. Nair, P.K. Nair, *Mod. Phys. Lett. B* **17**, 609 (2001).

[27] B.J. Zheng, J.S. Lian, L. Zhao, Q. Jiang, *Appl. Surf. Sci.* **256**, 2910 (2010).

[28] F. Yakuphanoglu, M. Caglar, Y. Caglar, S. Ilican, *J. Alloys Comp.* **506**, 188 (2010).

[29] C.V. Suryanarayana, *Bull. Electrochem.* **2**, 57 (1986).

[30] M.D. Uplane, P.N. Kshirsagar, B.J. Lokhande, C.H. Bhosale, *Mater. Chem. Phys.* **8630**, 1 (1999).

[31] L.M. Peter, *J. Electroanal. Chem.* **98**, 49 (1979).

[32] Y. Yang, L. Wang, H. Yan, S. Jin, T.J. Marksa, S. Li, *Appl. Phys. Lett.* **89**, 051116 (2006).

[33] M. Yan, M. Lane, C.R. Kannewurf, R.P.H. Chang, *Appl. Phys. Lett.* **78**, 2342 (2001).

[34] B.J. Zheng, J.S. Lian, L. Zhao, Q. Jiang, *Vacuum* **85**, 861 (2011).

[35] T.J. Coutts, D.L. Young, X. Li, W.P. Mulligan, X. Wu, *J. Vac. Sci. Technol. A* **18**, 2646 (2000).

[36] A.W. Metz, J.R. Ireland, J.G. Zheng, R. Lobo, Y. Yang, J. Ni, C.L. Stern, C.V.P. Dravid, N. Bontempz, C.R. Kannewurf, K.R. Poeppelmeier, T.J. Marks, *J. Am. Chem. Soc.* **126**, 8477 (2004).

[37] R. Kumaravel, S. Menaka, S. Regina Mary Snega, K. Ramamurthi, K. Jeganathan, *Mater. Chem. Phys.* **122**, 444 (2010).

[38] J.C. Manifacier, *Thin Solid Films* **90**, 297 (1982).

[39] B. Saha, R. Thapa, K.K. Chattopadhyay, *Solid State Commun.* **145**, 33 (2008).

[40] P.H. Jefferson, S.A. Hatfield, T.D. Veal, P.D.C. King, C.F. McConville, J. Zuniga-Perez, V. Munoz-Sanjose, *Appl. Phys. Lett.* **92**, 022101 (2008).

[41] Y.S. Choi, C.G. Lee, S.M. Cho, *Thin Solid Films* **289**, 153 (1996).

[42] J.S. Cruz, G.T. Delgado, R.C. Perez, S.J. Sandoval, O.J. Sandoval, C.I.Z. Romero, J.M. Marin, O.Z. Angel, *Thin Solid Films* **493**, 83 (2005).

[43] R.M. Navarro, F. del Valle, J.L.G. Fierro, *Int. J. Hydrog. En.* **33**, 4265 (2008).

[44] A.A. Dakhel, *Semicond. Sci. Technol.* **23**, 055017 (2008).

[45] R. Kondo, H. Okhimura, Y. Sakai, *Jpn. J. Appl. Phys.* **10**, 1547 (1971).

[46] S. Aksoy, Y. Caglar, S. Ilican, M. Caglar, *Int. J. Hydrog. En.* **34**, 5191 (2009).

[47] M. Ortega, G. Santana, A. Morales-Acevedo, *Solid State Electron.* **44**, 1765 (2000).

[48] D.M.C. Galicia, R.C. Perez, O.J. Sandoval, S.J. Sandoval, G.T. Delgado, C.I.Z. Romero, *Thin Solid Films* **371**, 105 (2000).

[49] R.J. Deokate, S.V. Salunkhe, G.L. Agawane, B.S. Pawar, S.M. Pawar, K.Y. Rajpure, A.V. Moholkar, J.H. Kim, *J. Alloys Comp.* **496**, 357 (2010).

[50] H. Finnkenrath, H. Kohler, M. Lochmann, Z.F. Angew, *Physic A* **21**, 512 (1966).

[51] K. Maschke, U. Rossler, *Phys. Status Solidi* **28**, 577 (1968).

[52] S. Tewari, *Solid State Commun.* **12**, 437 (1973).

[53] A. Breeze, P.G. Perkins, *Solid State Commun.* **13**, 1031 (1973).

[54] A.A. Dakhel, *Solar Energy* **82**, 513 (2008).

[55] J. Arthur Nozik, *Nano Lett.* **10**, 2735 (2010).

[56] V. Prashant Kamat, *J. Phys. Chem. C* **112**, 18737 (2008).

[57] C.C. Vidyasagar, Y. Arthoba Naik, T.G. Venkatesh, R. Viswanatha, *Powder Technol.* **214**, 337 (2011).

[58] M.A. Flores, R. Castanedo, G. Torres, O. Zelaya, *Sol. En. Mater. Sol. Cells* **93**, 28 (2009).

[59] J.S. Cruz, G.T. Delgado, R.C. Perez, S.J. Sandoval, J.M. Marin, O.Z. Angel, *Sol. En. Mater. Sol. Cells* **90**, 2272 (2006).

[60] C.S. Ferekides, R. Mamazza, U. Balasubramanian, D.L. Morel, *Thin Solid Films* **480**, 224 (2005).

[61] C. Xiangfeng, *Mater. Res. Bull.* **38**, 1705 (2003).

[62] M. Ristic, S. Popovic, S. Music, *Mater. Lett.* **58**, 2494 (2004).

[63] T.L. Chu, S.S. Chu, *J. Electron. Mater.* **19**, 1003 (1990).

[64] R.S. Mane, S.H. Han, *Electrochem. Commun.* **7**, 205 (2005).

[65] F.Z. Wang, Z.Z. Ye, D.W. Ma, L.P. Zhu, F. Zhuge, H.P. He, *Appl. Phys. Lett.* **87**, 1443101 (2005).

[66] F.Z. Wang, H.P. He, Z.Z. Ye, L.P. Zhu, *J. Appl. Phys.* **8**, 084301 (2005).

[67] A. Wang, J.R. Babcock, N.L. Edleman, A.W. Metz, M.A. Lane, R. Asahi, V.P. Dravid, C.R. Kannewurf, *Proc. Natl. Acad. Sci.* **98**, 7113 (2001).

[68] B. Li, L. Zeng, F. Zhang, *Phys. Status Solidi A* **201**, 960 (2004).

[69] H.M. Ali, H.A. Mohamed, M.M. Wakkad, M.F. Hasaneen, *Thin Solid Films* **515**, 3024 (2007).

[70] J. Santos Cruz, G. Torres Delgado, R. Castanedo Pérez, C.I. Zúñiga Romero, O. Zelaya Angel, *Thin Solid Films* **515**, 5381 (2007).

[71] P.K. Ghosh, R. Maity, K.K. Chattopadhyay, *Sol. En. Mater. Sol. Cells* **81**, 279 (2004).

[72] C. Aydın, H.M. El-Nasser, F. Yakuphanoglu, I.S. Yahia, M. Aksoy, *J. Alloys Comp.* **509**, 854 (2011).

[73] B.K. Sonawane, Vrushali Shelke, M.P. Bhole, D.S. Patil, *J. Phys. Chem. Solids* **72**, 1442 (2011).

[74] R.K. Gupta, F. Yakuphanoglu, F.M. Amanullah, *Physica E* **43**, 1666 (2011).

[75] Y. Yang, S.J. Shu, J.E. Medvedeva, J.R. Ireland, A.W. Metz, Ni. Jun, M.C. Hersam, A.J. Freeman, T.J. Marks, *J. Am. Chem. Soc.* **127**, 8796 (2005).

[76] A.A. Dakhel, *J. Alloys Comp.* **475**, 51 (2009).

[77] R.S. De Biasi, M.L.N. Grillo, *J. Alloys Comp.* **485**, 26 (2009).

[78] R. Maity, K.K. Chattopadhyay, *Sol. En. Mater. Sol. Cells* **90**, 597 (2006).

[79] R.J. Deokate, S.M. Pawar, A.V. Moholkar, V.S. Sawant, C.A. Pawar, C.H. Bhosale, K.Y. Rajpure, *Appl. Surf. Sci.* **254**, 2187 (2008).

[80] F. Yakuphanoglu, *Solar Energy* **85**, 2704 (2011).

[81] A.A. Dakhel, *J. Mater. Sci.* **46**, 1455 (2011).

[82] A.A. Dakhel, *Sol. Energy* **83**, 934 (2009).

[83] R.K. Gupta, K. Ghosh, R. Patel, P.K. Kahol, *Appl. Surf. Sci.* **255**, 6252 (2009).

[84] R.K. Gupta, K. Ghosh, R. Patel, S.R. Mishra, P.K. Kahol, *Mater. Lett.* **62**, 4103 (2008).

[85] R.K. Gupta, K. Ghosh, R. Patel, S.R. Mishra, P.K. Kahol, *Appl. Surf. Sci.* **254**, 5868 (2008).

[86] R.K. Gupta, K. Ghosh, R. Patel, S.R. Mishra, P.K. Kahol, *Curr. Appl. Phys.* **9**, 673 (2009).

[87] E. Martin, M. Yan, M. Lane, J. Ireland, C. Kannewurf, R.H. Chang, *Thin Solid Films* **461**, 309 (2004).

[88] M. Yan, M. Lane, C.R. Kannewurf, R.P.H. Chang, *Appl. Phys. Lett.* **78**, 02342 (2001).

[89] E. Burstein, *Phys. Rev.* **93**, 632 (1954).

[90] F. Yakuphanoglu, *Appl. Surf. Sci.* **257**, 1413 (2010).

[91] A.A. Dakhel, *Thin Solid Films* **517**, 886 (2008).

[92] R.J. Deokate, S.V. Salunkhe, G.L. Agawane, B.S. Pawar, S.M. Pawar, K.Y. Rajpure, A.V. Moholkar, J.H. Kim, *J. Alloys Comp.* **496**, 357 (2010).

[93] *Optical Properties of Solids*, Ed. F. Abeles, North-Holland, Amsterdam 1972.

[94] M. DiDomenico, S.H. Wemple, *J. Appl. Phys.* **40**, 720 (1969).

[95] B. Gunduz, F. Yakuphanoglu, *Sensors Actuat. A* **178**, 141 (2012).

[96] G. Yogeeswaran, C.R. Chenthamarakshan, A. Seshadri, N.R. de Tacconi, K. Rajeshwar, *Thin Solid Films* **515**, 2464 (2006).

[97] A.K. Wolaton, T.S. Moss, *Proc. R. Soc.* **81**, 5091 (1963).

[98] W.G. Spitzer, H.Y. Fan, *Phys. Rev.* **106**, 882 (1957).

[99] J. Taue, in: *Optical Properties of Solids*, Ed. F. Abeles, North-Holland, Amsterdam 1972.

[100] J.N. Hodgson, *Optical Absorption and Dispersion in Solids*, Chapman and Hall, London 1970.